BALL BROTHERS RESEARCH CORPORATION

BOULDER, COLORADO

Final Report

WOLF TRAP CONTINUATION STUDY

Prepared for
University of Rochester

Contract No. NsG209-AG1

F67-13 5 Oct 1967

PREPARED

F. Burlingame
Staff Scientist

D. Buckendahl
Project Engineer

APPROVED

R. E. Hathaway
Program Manager

FORM BR-72A

FOREWORD

This report has been compiled for the University of Rochester under agreement NsG-209 AG-1, Modification 4, entitled "Wolf Trap Microbe Detection Device" and constitutes the final report on the Wolf Trap experiment continuation study.

The authors gratefully acknowledge major contributions from Margo Shaw, research analyst, and June Warwick, technical editor.

ABSTRACT

In 1963, the hardware development of the Wolf Trap detection device began, culminating in an engineering model in 1966. The resulting device is patterned after the early work of Dr. Vishniac, who provided information on light scattering and pH changes in an enrichment culture. The original design effort was simply to transform a laboratory technique into something suitable for a space mission—with no attempt to augment the original "yes/no" indication of life.

After the device was built and tested, it became possible to critically evaluate the *conclusiveness* of the data provided by the Wolf Trap. Light scattering is a powerful tool in the detection of life, providing direct observation of increases in the number of suspended organisms. Present day technological deficiencies in pH probe manufacture has caused us to consider alternate measurements of chemical changes caused by biological activity. These alternatives are sought because it is realized that to insure meaningful data, both an increase in particle number and changes in biological activity must be measured.

This report reviews the theory of light scattering, X-ray scattering, conductivity, and fluorescence. A discussion follows each theoretical section to stress those aspects of theory which should be considered in future decisions on Wolf Trap. Thus, an alternative to pH measurement is examined in theory, then discussed in relationship to the goal of current work on Wolf Trap—to insure that the data obtained by the Wolf Trap device is conclusive.

CONTENTS

ILLUSTRATIONS

Section 1
LIGHT SCATTERING

Before presenting the theory of light scattering, it may be well to review its historical development. In 1868, John Tyndall presented a paper to the Royal Society of London in which he explained the blueness of the sky as a function of the size and density of particles in the air. Shortly afterward, Lord Rayleigh made the first scientific attempts to measure light scattering. After Maxwell introduced his electromagnetic concepts and developed equations to explain the behavior of light, rigorous mathematical treatment of light scattering and other light phenomena became possible. Within a few years, Debye and Mie together succeeded in finding practical mathematical solutions to the very involved theoretical equations set forth by Maxwell. At first they worked with the simplified model of Rayleigh and considered only scatter from very small spherical particles. Later, they extended the basic theory to include a wider range of particle sizes. They also evaluated the effect of refractive index and other physical properties of particles. However, large electronic computers were required before full advantage could be taken of much of this work. Today, the literature contains computer treatments of many special cases based upon the early concepts by Debye and Mie.

Very recently, biochemists and polymer chemists have applied light scattering techniques to the problem of determining molecular shapes and dimensions. This exacting work requires the use of highly specialized instruments. Commercial products do not meet the need, forcing researchers to either modify existing instruments, or develop their own. The commercial instruments are designed primarily for determining crude size distribution of particulate matter, and are used in studies of atmospheric and water contamination. This is far afield of the researcher's interest in the physical properties of single particles.

If a beam of unpolarized parallel light is passed through a suspension of small nonabsorbing particles, light is scattered from the path of the beam and the suspension appears cloudy. From this, it can be concluded that the suspended particles have a refractive index different from that of the medium.

In a unit volume of solvent, all solvent molecules are theoretically of equal size and arranged in a three-dimensional, regular array. When a beam of parallel, nonpolarized light passes through the liquid, each molecule acts as a center of scatter. All of the light scattered in directions lateral to the incident beam is cancelled by destructive interference. Only those photons that are scattered parallel to the incident beam are reinforced by constructive interference. To the observer, all of the light has been scattered in the forward direction.

However, an inhomogeneity upsets this condition and produces lateral scattering. Therefore, when particles are introduced into the hypothetical solvent in a random fashion, the particles produce inhomogeneities and become centers of scatter. The lateral scattering attenuates the intensity of the incident beam as it passes through the inhomogeneous medium.

This attenuation of the primary light beam intensity in a dilute suspension is shown by the equation

$$I = I_o e^{-\tau X} \qquad (1.1)$$

Where I_o is the intensity of the primary beam, I is the intensity after the light has penetrated X distance into the suspension, and τ is the reciprocal of the distance through which the incident beam must pass in order to be weakened by scattering to 1/e or 43 percent of I_o. In a suspension of small particles (diameter 0.1 microns) such as we are considering, this distance is

about 100 meters; therefore, τ is of the order of $1/10^2$ meters. In general τ is the function of a variety of factors: the wavelength of the primary light, the concentration, the size, the shape, and the relative refractive index of the scattering particle.

Equation (1.2) shows the fraction of the incident light that is scattered by a unit volume of the suspension

$$\tau = \frac{8\pi}{3}\left(\frac{2\pi}{\lambda}\right)^4 n\alpha^2 \qquad (1.2)$$

where n is the number of particles per cubic centimeter, λ is the wavelength of the incident light, and α is a proportionality factor relating the magnitude of the induced electric moment to the strength of the exciting electric field. Each particle radiates as an independent dipole that oscillates in phase with the incident ray. The dipole is created when one or more of the electrons in a particle are set into forced vibration by the incident light. This oscillating dipole immediately returns to normal by radiating a secondary wave of the same frequency as the incident light.

In the special case of small spherical particles, α of Eq. (1.2) is proportional to the volume of the particle. The intensity of the scattered light is therefore proportional to the square of the volume or to the sixth power of the radius of the particle. Within the particle size range (diameter less than 1/10 λ) for which the Rayleigh equation holds true, there is thus this pronounced effect on the intensity of the scattered light as a function of the particle size.

Another factor affecting the intensity of the scattered light is n of Eq. (1.2). In other words, as the concentration of particles in a solution increases, τ increases proportionately.

For any angle θ measured from the direction of the incident beam, the intensity of the observed scattered light is the result of all of the constructive and destructive interactions of the light waves (Fig. 1-1). For systems obeying the Rayleigh equation, the observed intensity of the scattered light is proportional to $(1 + \cos^2\theta)$; that is, τ_θ is dependent on the magnitude of angle θ.

In this case, Eq. (1.2) becomes

$$\tau_{ob} = \frac{8\pi}{3}\left(\frac{2\pi}{\lambda}\right)^4 n\alpha^2 \quad (1 + \cos^2\theta) \qquad (1.3)$$

where τ_{ob}, the observed turbidity, for any θ now relates to that fraction of the incident light scattered by angle θ. The scattered light is in fact composed of two optically polarized components. One component has the electric vector perpendicular to the axis of the incident beam, the electric vector of the other is parallel to this axis.

Figures 1-2 through 1-8 are semi-log polar plots of angular scattered intensity.* In these figures, a solid line represents

*Figures 1-2 through 1-7 are obtained by plotting data from computer solutions of Mie theory equations published by NBS: "Tables of Scattering Functions For Spherical Particles", U.S. National Bureau of Standards, Applied Mathematics Series (AMS) No. 4, U.S. Government Printing Office, Jan 25 1949. Figure 1-8 is from G. C. Clark, Chiao-Min Chu, and S. W. Churchill, "Angular Distribution Coefficients For Radiation Scattered by a Spherical Particle." Journal of the Optical Society of America, Vol. 47, pp. 81 to 84 1957.

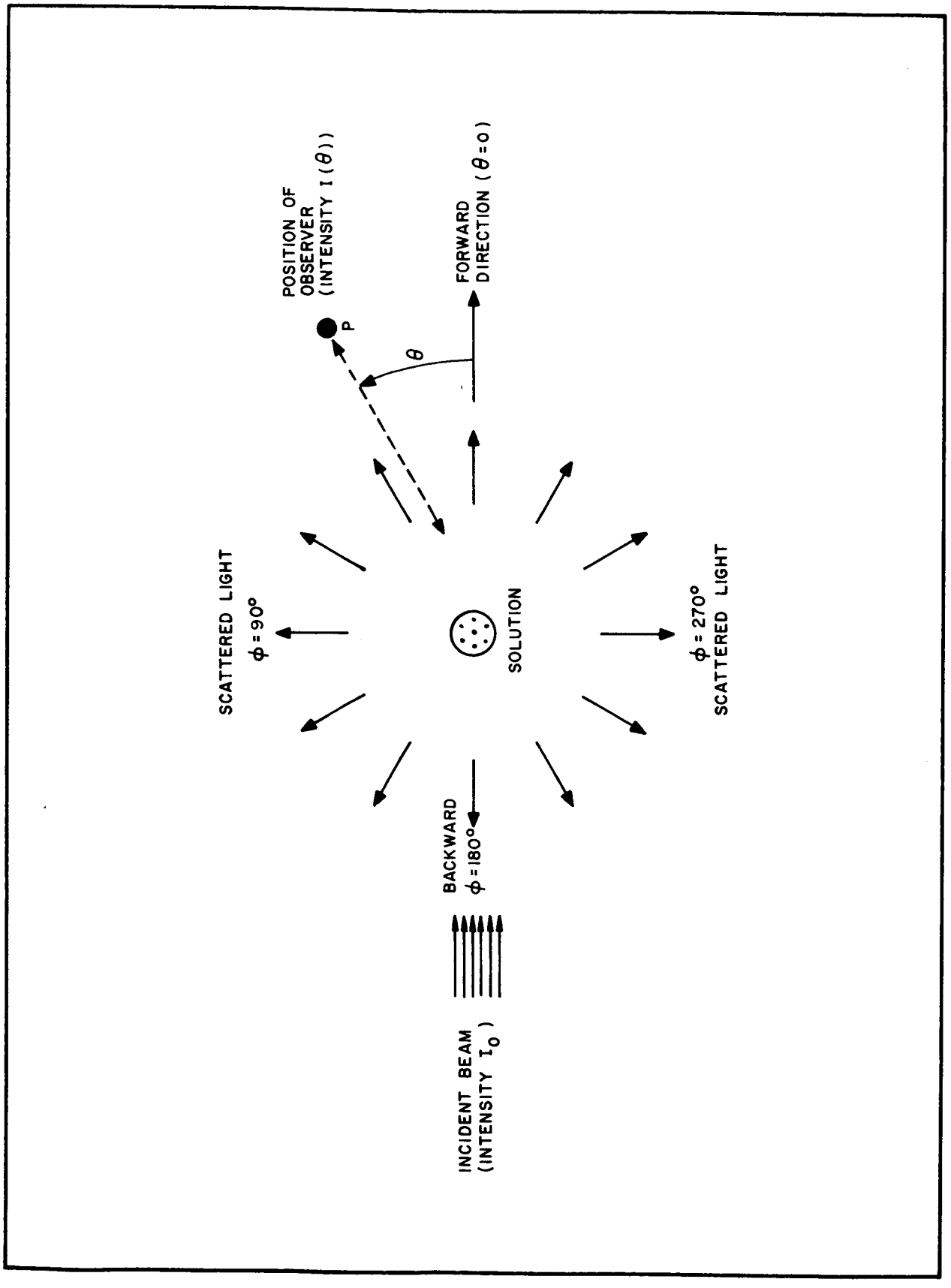

Fig. 1-1 Light Scattering Model

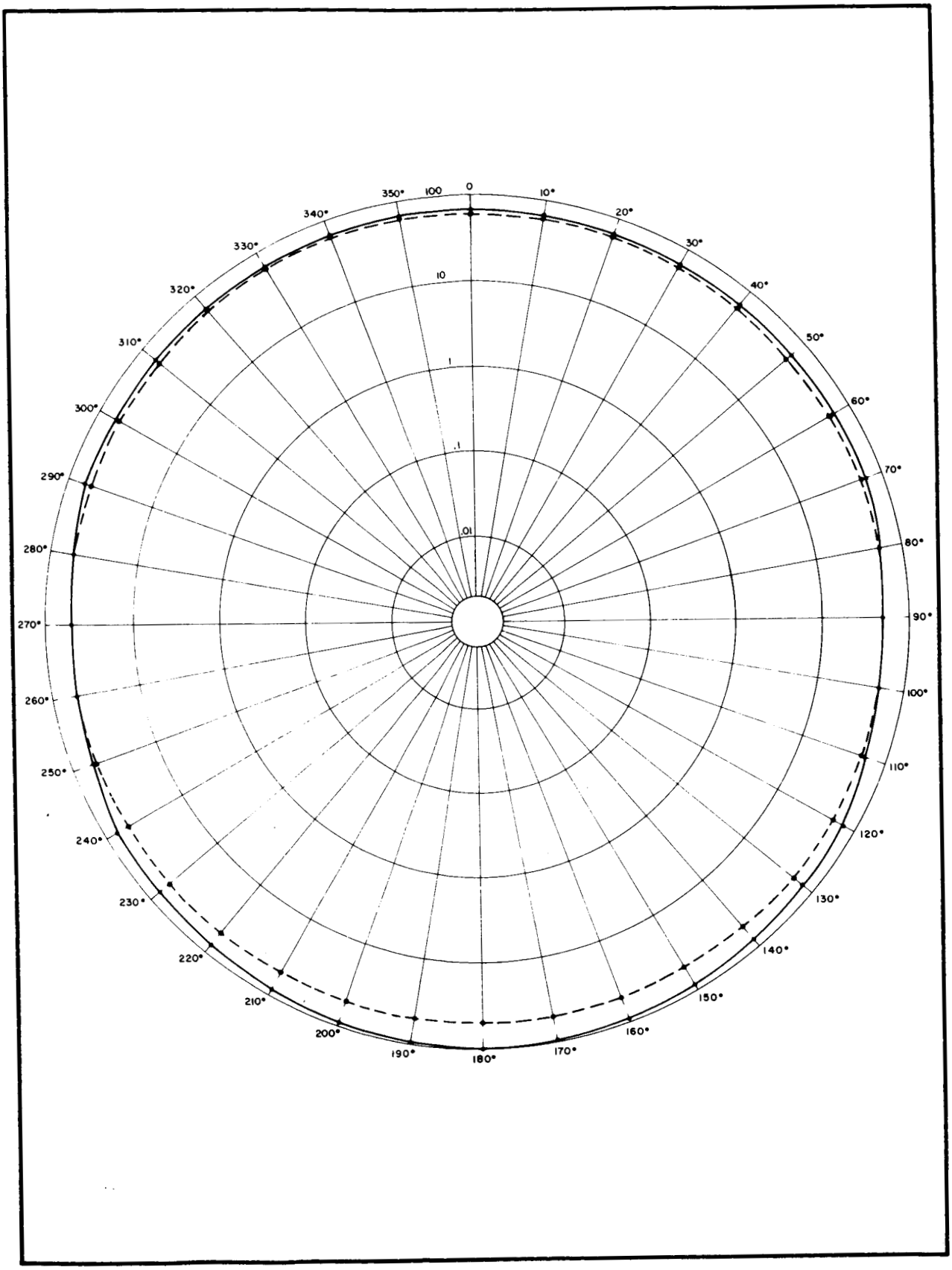

Fig. 1-2 Small Spherical Dielectric Scatter Plot: m = 1.33; α = 0.5

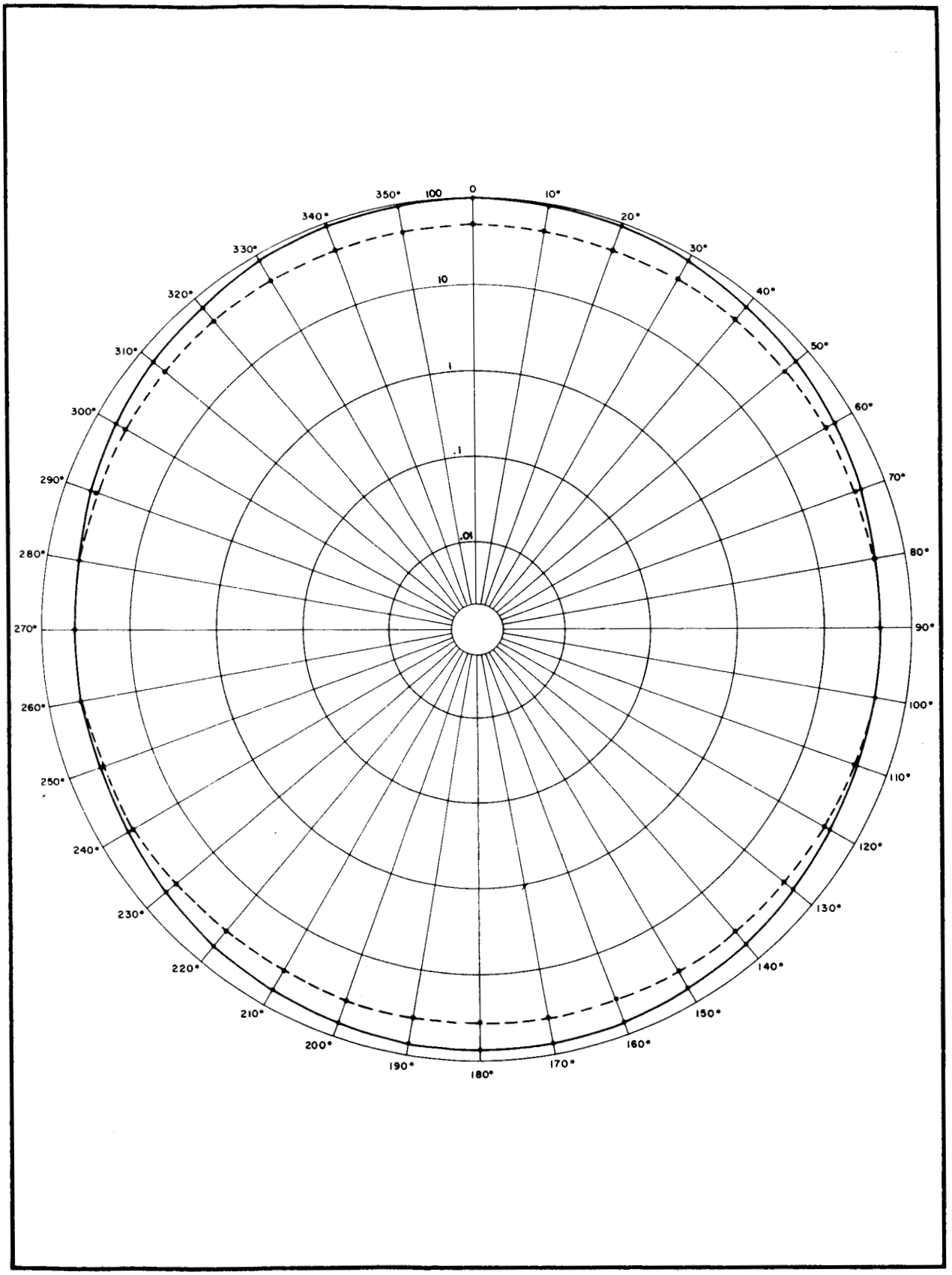

Fig. 1-3 Small Spherical Dielectric Scatter Plot: m = 2.0; α = 0.5

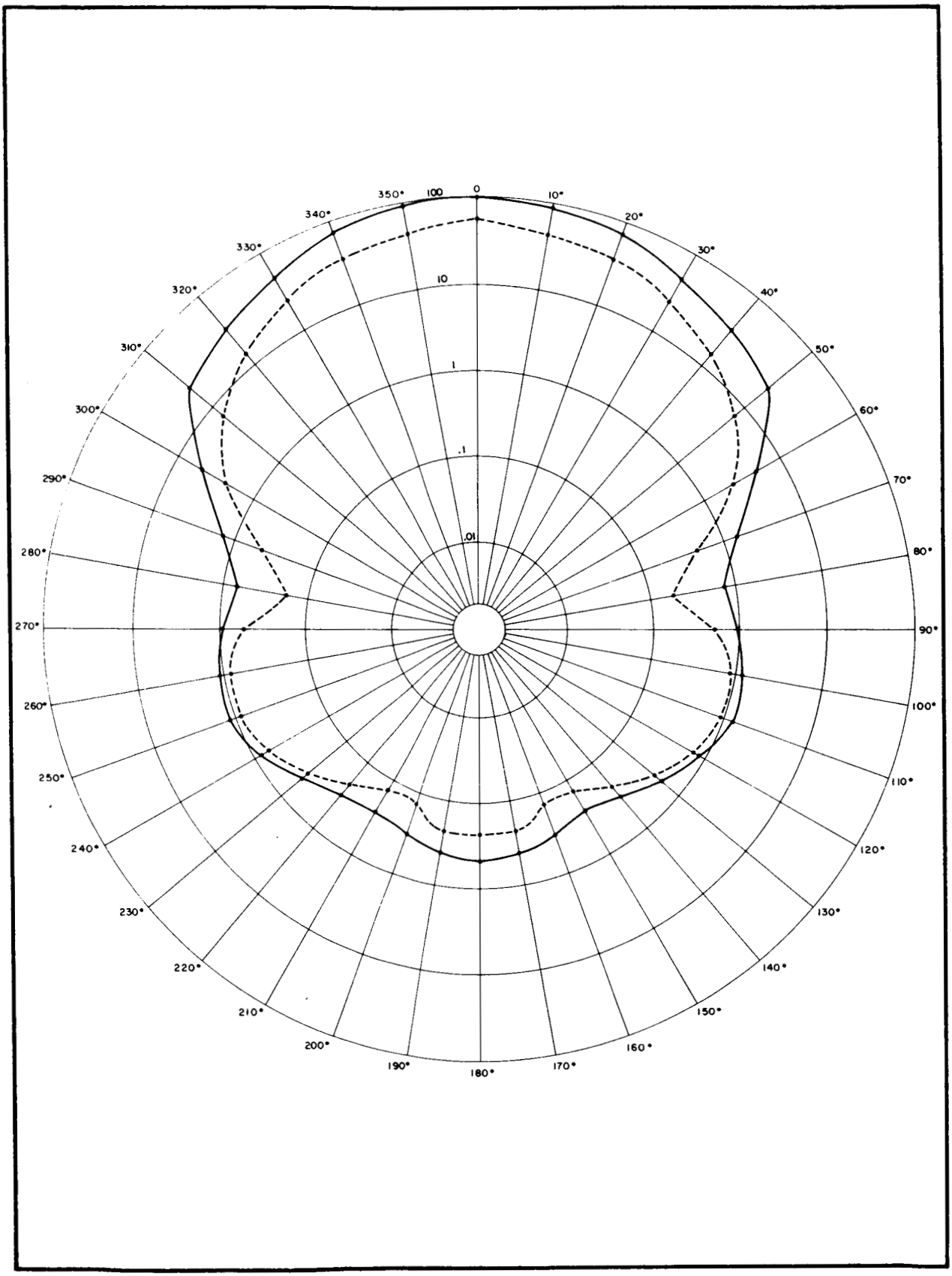

Fig. 1-4 Spherical Dielectric Scatter Plot: m = 1.33; α = 3.0

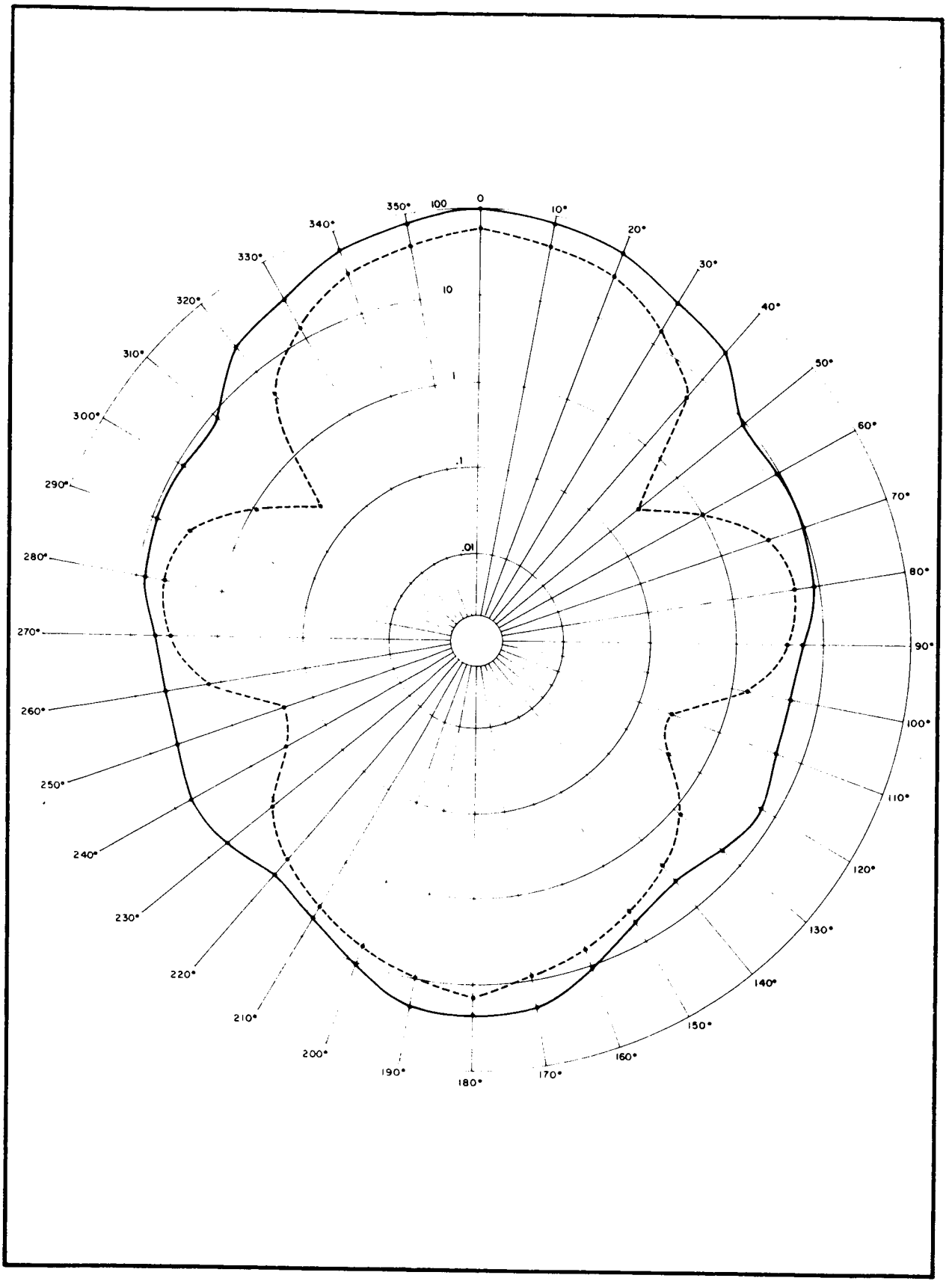

Fig. 1-5 Spherical Dielectric Scatter Plot: m = 2.0; α = 3.0

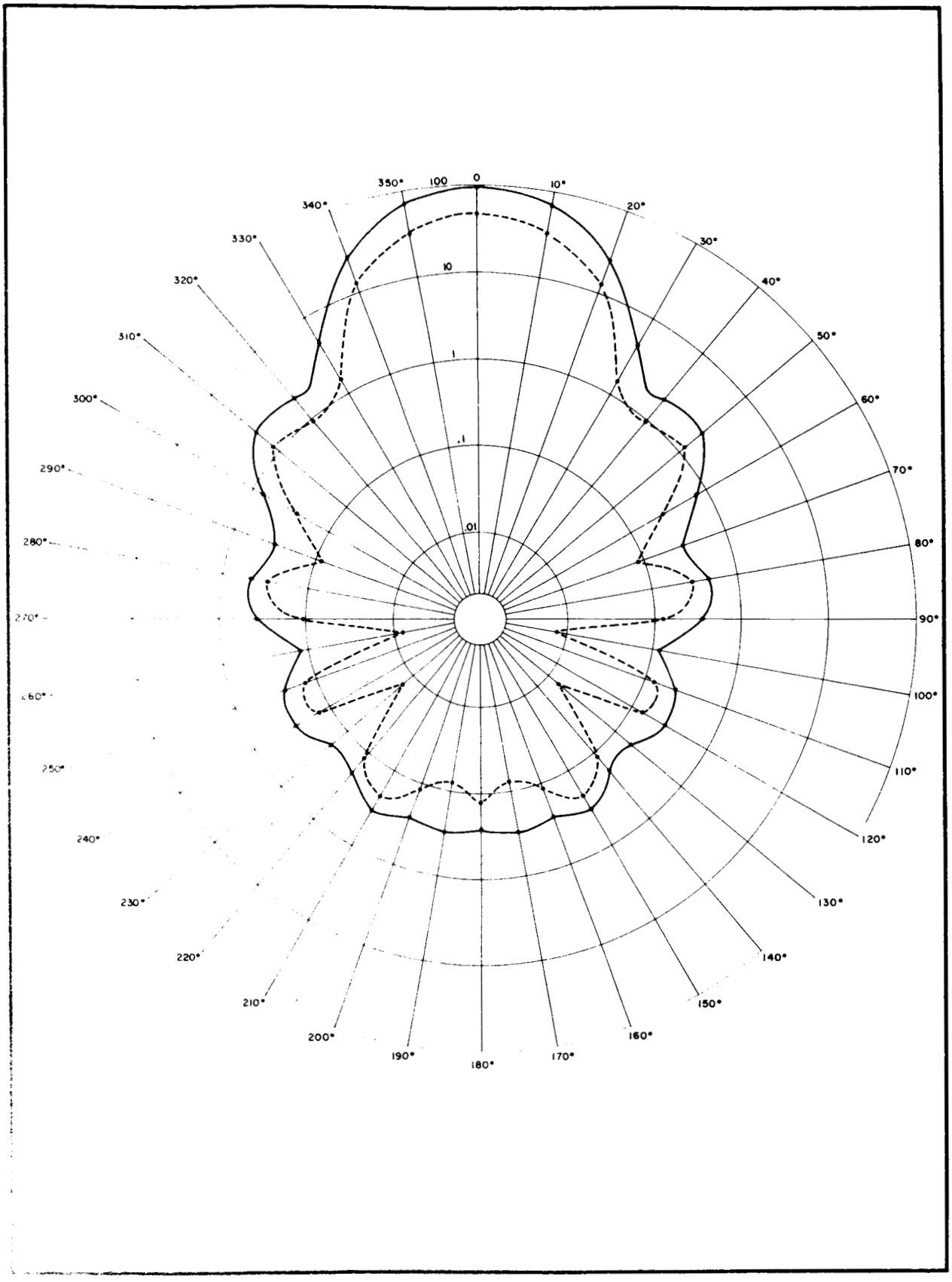

Fig. 1-6 Spherical Dielectric Scatter Plot: m = 1.33; α = 6.0

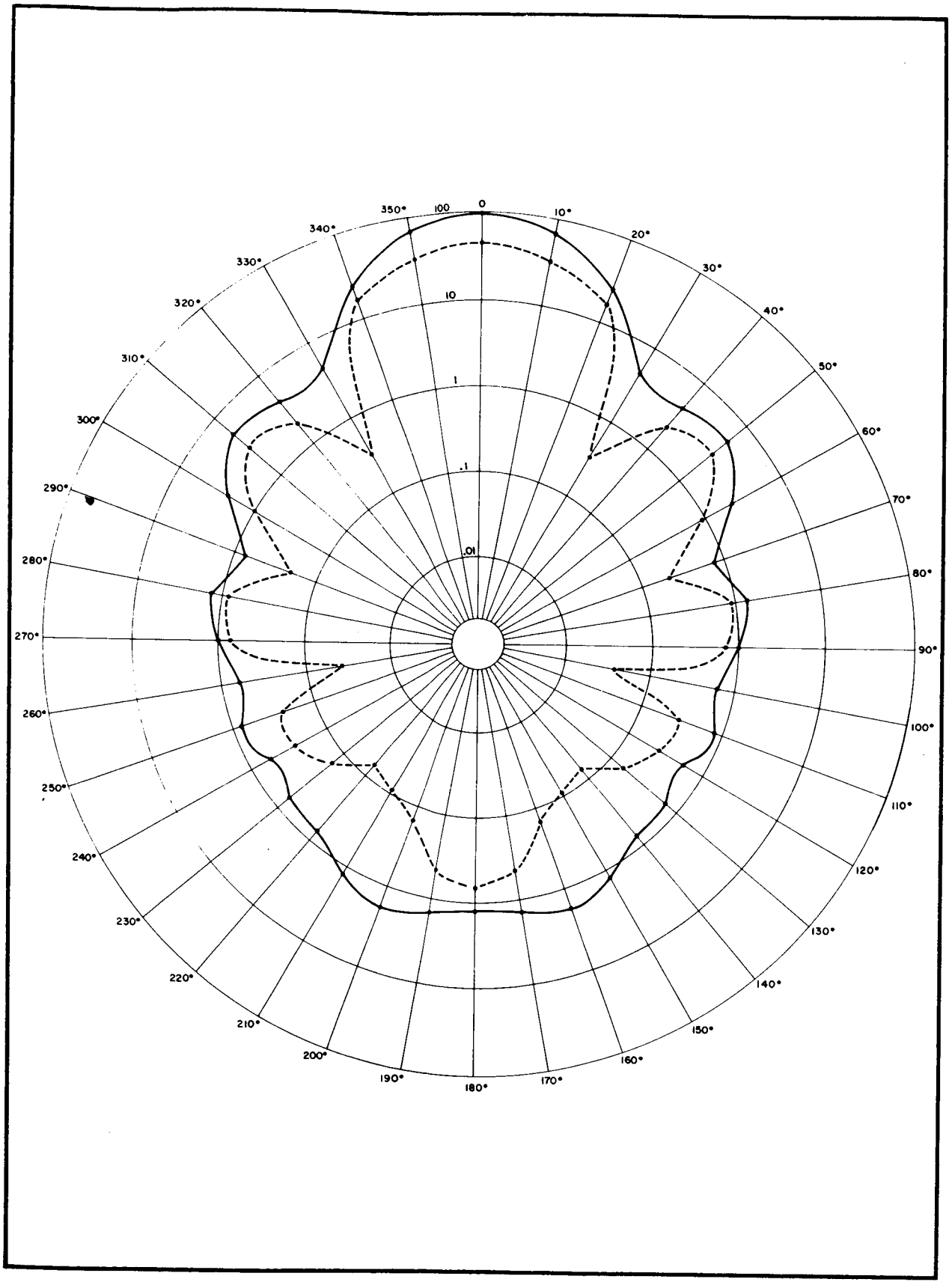

Fig. 1-7 Spherical Dielectric Scatter Plot: m = 2.0; α = 6.0

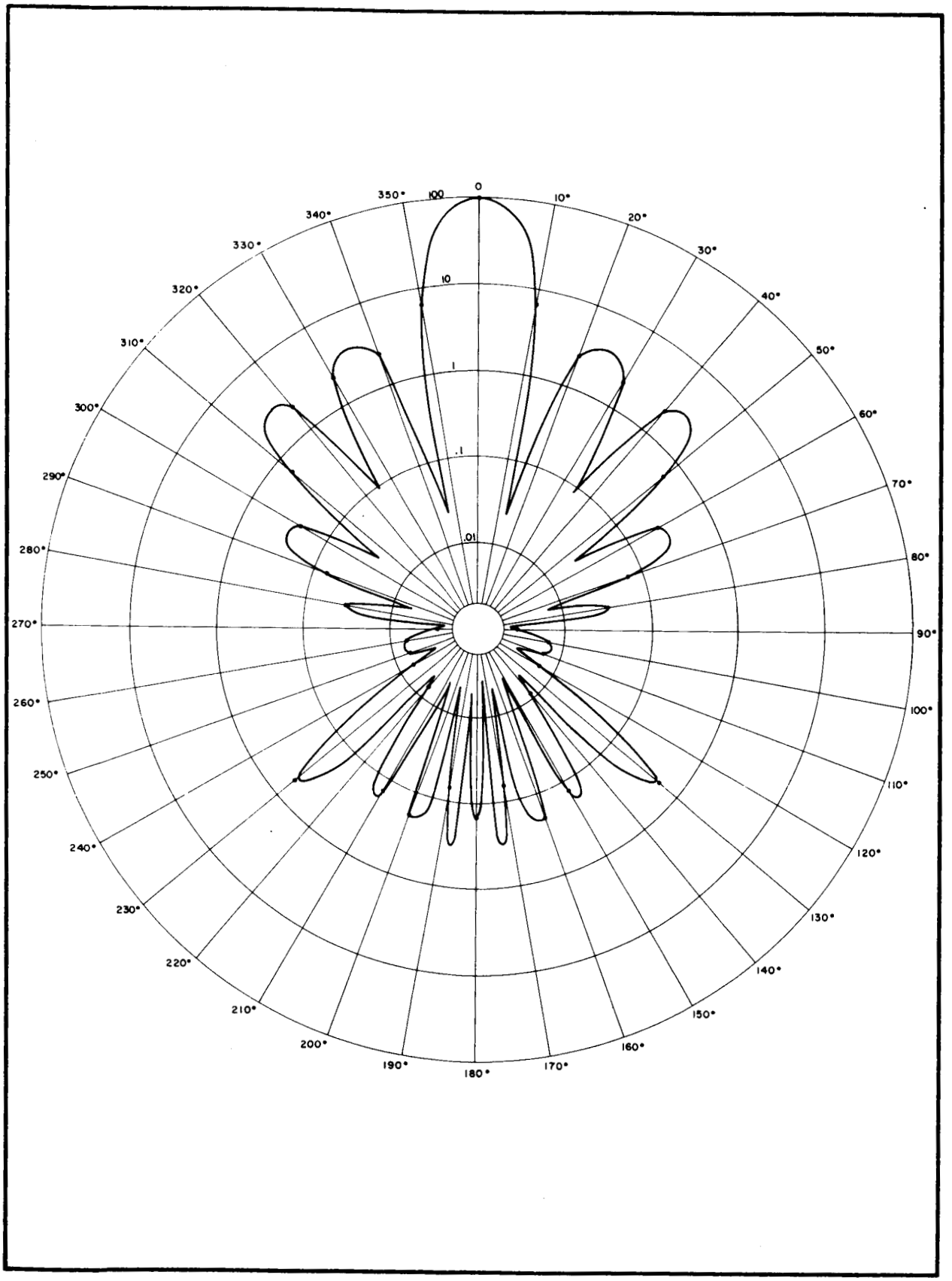

Fig. 1-8 Large Spherical Dielectric Scatter Plot: m = 1.33; α = 25

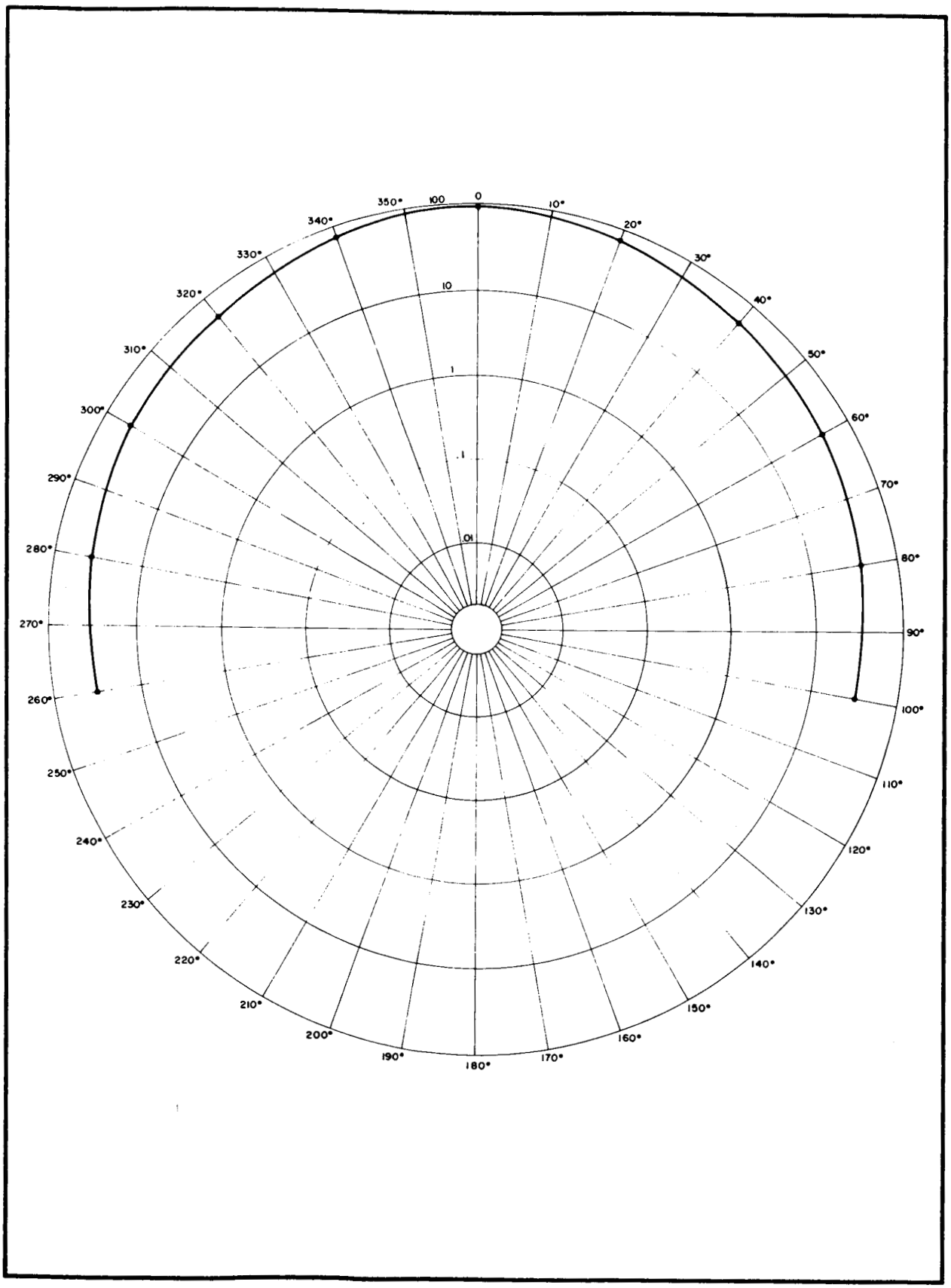

Fig. 1-9 Rod-Like Particle Scatter Plot: m ~ 2; α = 3

the total scattered light intensity. The broken line represents only that component in which the electric vector is perpendicular to the axis of the incident beam. This second line shows that there is a difference in intensity as a function of θ and optical polarization as a function of θ for each of the two components. Alpha—as found on these figures—is defined as

$$\alpha = \frac{\pi \ell}{\lambda} \tag{1.4}$$

where ℓ is the length of the particle. It should not be confused with the alpha of Eq. (1.2).

Also, the m that appears with these figures is the relative refractive index of the system

$$m = \frac{i_1}{i_0} \tag{1.5}$$

where i_1 is the refractive index of the particle, and i_0 is the refractive index of the solvent. All of these terms appear in Mie theory equations.

Figures 1-2 and 1-3 represent the special case of small, spherical, nonabosrbing particles. Figures 1-4, 1-5, 1-6, and 1-7 are plotted from data for larger particles, (α approximately equal to or greater than 3.) The angular scattering patterns for these larger particles exhibit pronounced maxima and minima. This can be attributed to destructive interference caused by multiple scattering points within each individual large particle. Rayleigh scatter simplifications do not hold in this particle size range, so that the equations that must be employed become very complex.

Looking at Fig. 1-2, 1-4, 1-6, and 1-8, it is noticed that as α increases for a given refractive index (here 1.33), the plots become more structured. In other words, as the particle size increases, the number of maxima and minima increases as does also the ratio of the intensity at one maximum to the intensity at the next minimum. In addition, the light scatter envelope varies from almost equal scatter in all directions, to a pronounced scatter in the forward direction.

Turning to a comparison of Figs. 1-2, 1-3, 1-4, 1-5, and 1-6, 1-7, where α is held constant for each pair, it is seen that a difference in refractive index (here we are comparing $m = 1.33$ and $m = 2.0$) causes very little change in the structure of the plot.

So far, we have considered light scatter for spherical, nonabsorbing particles. It should be noted that other cases exist. If the particles are light-absorbing, the overall intensity of scattered light is greatly reduced. However, an increase in the number of particles still produces an increase in the amount of light scattered, as in the case for nonabsorbing particles. If the particles are large and light-absorbing, the light scatter diagrams show less pronounced maxima and minima. It has been suggested that this is due to the attenuation of internally reflected rays by the absorbing material, which provides less opportunity for destructive interference to occur. If the spheres reflect light, back scatter (where $\theta = 180$ degrees) is greatly increased.

Figure 1-9 is a partial light scatter diagram for rod-like particles. The smooth appearance of this partial plot should be compared with Figs. 1-4 and 1-5.

These three diagrams might be expected to be very similar—since the alpha for each plot is the same. However, another consideration must be introduced: the three plots are for random orientation of particles in a suspension. Because a rod has a long and short axis, we can speak of random and nonrandom orientation of all such particles in a suspension. And spheres by definition, cannot be said to be in random or nonrandom orientation since they appear the same from all directions.

If a light scatter plot were made for nonrandom orientation of rod-like particles, the plot would be highly structured—unlike Fig. 1-9.* In contrast, there is no change in the structure of a light scatter plot as a function of orientation for spheres, due to their geometry.

Furthermore, Powell** recently has shown that when rod-like particles are oriented so that the long axis is normal to the incident beam, the intensity of scattered light is increased by 28 percent over that observed for random orientation. Similar experiments with human erythrocytes resulted in a 12 percent increase.

---

*Figure 1-9 is from Gerald Oster, P. M. Doty and B. M. Zimm, "Light Scattering Studies of Wbacco Mosaic Virus," J. Am. Chem. Soc., Vol. 69, pp. 1193 to 1197, 1967.

**E. O. Powell and P. J. Stoward, "A Photometric Method for Following Changes in Length of Bacteria," Journal of General Microbiology, Vol. 27, pp. 489 to 500, 1962.

In light of the preceding theoretical work, let us consider the requirements that must be met in detecting life. The following is a familiar list:

(1) The technique used in life detection should be based on the fewest assumptions possible.

(2) Data that is interpreted as a positive indication of life should have a low probability of occurrence if there is no life present.

(3) A negative indication of life should be as conclusive as possible.

Life can be characterized as that which reproduces, mutates, and reproduces mutations. The approach used in Wolf Trap rests on this basic assumption—that life on Mars does reproduce. The preliminary engineering model has been tested to prove that the Wolf Trap technique is basically sound. It is now only necessary to optimize the design of the instrument as advances in components allow.

In theory, a nutrient solution alone scatters no light. When particles are introduced, a fraction of the incident light τ is scattered.

$$\tau = \frac{8\pi}{3}\left(\frac{2\pi}{\lambda}\right)^4 n\alpha^2 \qquad (6.1)$$

This τ varies as n and/or α vary. It is at this point that we should consider requirement (2). A series of calibration curves for many different organisms and combinations of organisms can be obtained in the laboratory with the Wolf Trap device. Experience gained in recognizing growth curves will insure that any chance increase in α is not misinterpreted as an increase in the number of organisms. Even if an increase in α were to approximate a growth curve, the measurement of other parameters would alleviate any confusion.

Light scatter theory indicates that the structure of a light scatter plot can provide an approximate size of spherical particles. This measurement becomes more significant if pure cultures are obtained. And an increase in the number of detectors could further refine this approximation.

A pure culture offers more, though, than a refined process of approximating particulate size. For example, if the organisms were to be oriented in an orderly arrangement after they have been identified as a pure culture, an approximation of their shape would also be possible.

So far we have been reviewing the theoretical potentials of the Wolf Trap device. There are many specific questions to be answered, and there are many alternatives to consider. Our next step should be laboratory testing. The following is a list of approaches that we feel would be advantageously tested.

(1) Multiple detectors would enable us to detect not only forward scatter but also scatter at other angles. Such a geometric arrangement would make both particle size and particle shape determinations possible.

(2) The path length of the light within the culture chamber could be increased, if this light could be reflected from the interior walls of the chamber. Such an increase in path length would intensify the signal strength for a given power expenditure.

(3) Pulsing the light source would reduce the power expenditure. Pulse amplifiers would improve the signal-to-noise ratio.

(4) It may be advantageous to detect life at the surface of the culture chamber (as well as within the nutrient media).

(5) It may be that the sun could provide an intense, broadband source of light.

(6) A light source suitable both for photosynthesis and light scatter measurement could greatly reduce power requirements.

(7) Fiber optics may provide a way to better distribute and direct the light from the light source.

(8) To aid in the determination of particle shape, it may be possible to orient the particles in an orderly arrangement (i.e., as blood cells in the capillaries) and stream the particles past the optics.

(9) A colorimeter determination may be possible

Section 2
X-RAY SCATTERING

In 1906, Charles Barkla and C. A. Sadler correctly determined the number of electrons in the carbon atom by measuring the X-ray scattering coefficient of carbon. This determination was based on the theoretical work of J. J. Thomson. Barkla's work formed a strong support for the supposition that X-rays are of the same nature as other known electromagnetic radiation.

In 1960, Kratky, Luzzati, Baro, and Witz used X-ray scattering techniques in an attempt to better understand the detailed structures of biopolymers in solution. In their work, they were able to determine molecular weight, particle density, volume, hydration, and surface to volume ratio for macromolecules.

We are basing our considerations of X-ray scattering as a complimentary technique of life detection on the Thomson equation

$$i_{el} = \frac{7.9 \times 10^{-26}}{a^2} P \frac{1 + \cos^2 2\Theta}{2} \qquad (2.1)$$

where i_{el} is the intensity of the scattered radiation when a single electron is exposed to a primary beam P of X-rays, a is the distance from the observer to the point of scatter, and 2Θ is the angle between the primary beam and the scattered radiation.

Basically, the phenomena of X-ray scattering and light scattering are identical. In other words, what applies to one in most cases, applies to the other. Two differences do arise, however, in the segments of the theory we are considering.

First, when working with light scatter, we were considering particles of 0.1μ to 1.0μ and wavelengths of 0.4 to 0.8μ (4000 to 8000 Å). Now we have turned our attention to macromolecules of approximately 0.01μ and wavelengths of 4.0 to 8.0×10^{-4}μ (1/1000 that of visible light).

Secondly, in the Thomson equation, we are now considering scatter from a single electron rather than from a whole particle. In light scatter, each particle radiates as an independent dipole oscillating in phase with the incident ray. The oscillating dipole immediately returns to normal by radiating a secondary wave of the same frequency as the incident light. In X-ray scatter, when a beam of electromagnetic radiation strikes an electron, some of the energy is absorbed and then reemitted at the same frequency as that of the incident radiation.

The reason for this second difference is historical. Rayleigh's work on light scatter was in terms of whole particles while Thomson's was in terms of single electrons, and these two view points have been continued in subsequent work in the field.

In light scatter, most of the scatter from a large particle is in the forward direction, as shown in Fig. 1-8. Macromolecules are so large in comparison to X-rays that, for all purposes, most of the X-rays are scattered in the forward direction. In theory, for a given α, a scatter plot looks the same whether $\ell = 0.1\mu$ or $\ell = 0.01\mu$ and λ is in the range of X-ray or visible light.

With this in mind, it can be seen that Θ, the angle between the primary beam and the scattered radiation, is always very small. Hence, the term $\frac{1 + \cos^2 2\Theta}{2}$ of Equation (2.1) approaches unity, and we need not consider it further. Our revised equation is

$$i_{el} = \frac{7.9 \times 10^{-26}}{a^2} \quad P \tag{2.2}$$

Let us now consider a substance of molecular weight M containing Z_1 mole-electrons per gram. When Z_1M electrons per molecule are exposed to a beam of X-rays, each electron acts as a diffraction center. The amplitude of these diffractions becomes additive, and the square of the resulting amplitude is proportional to the intensity. Therefore, Eq. (2.2) becomes

$$i_{el} = \frac{7.9 \times 10^{-26}}{a^2} \quad P\ Z_1^2M^2 \tag{2.3}$$

In a theoretical dispersed single component system, there is no phase relationship between the scattered rays if the average distance between the macromolecules is greater than ℓ, where ℓ is the dimension of a macromolecule. If the system contains g grams (i.e. $\frac{gN}{M}$ where N is Avagadro's number), then the scatter intensity is given by

$$i_{el} = \frac{7.9 \times 10^{-26}}{a^2} \quad PZ_1^2M^2\ \frac{gN}{M} \tag{2.4}$$

or

$$i_{el} = \frac{7.9 \times 10^{-26}}{a^2} \quad PZ_1MgN \tag{2.5}$$

This scatter intensity is proportional to the weight concentration of the system as well as to the weight of each molecule. This is similar to the effect of n in Eq. (1.2): i.e., as n increases, τ increases.

Since this single component system does not encompass the practical case of the nutrient solution that we must work with, our interest turns to the molecular dimensions of the solvent and solute particles. A uniform density of electrons throughout the solvent system is necessary so that the electrons of the solvent molecules appear as a continuum. As noted in the section on light scatter theory, X-rays scattered laterally from the nutrient will be extinguished by destructive interference. Ideally, the only inhomogeneities in the continuum are the macromolecules, which appear as localized disturbances. X-ray scattering occurs at these sites because the macromolecules have higher electron densities than do the molecules of the nutrient solution they have displaced.

This effect is described by the relationship

$$Z_e = Z_1 \cdot \bar{V}_1 P_2 \qquad (2.6)$$

Where Z_e is the excess electrons, Z_1 the effective mole-electrons per gram of macromolecular substance, and $\bar{V}_1$ the partial specific volume of the macromolecules. The electron density P_2 is the number of mole-electrons per cm^3 and is given by

$$P_2 = \text{density} \times \frac{\Sigma \text{ atomic number of solute}}{\Sigma \text{ atomic weight of solute}} \qquad (2.7)$$

where the term "density" reflects the fact that—due to the nature of bond lengths—a polymerized molecule occupies less space than an equivalent number of individual monomer molecules.

Let us return once again to the criteria that must be met in detecting life.

Both requirements (2) and (3) (page 1-17) stress the need for measuring additional parameters. Our previous work with the Wolf Trap device has indicated several useful and interesting possibilities. However, laboratory testing is necessary to evaluate these various approaches.

There are several major considerations governing the selection of the various parameters to be measured. These considerations include the power available, the weight, size, compatibility (with other experiments), ruggedness, and telemetry characteristics of the device.

X-ray scatter is similar to light scatter, except that X-rays are scattered by much smaller particles. Therefore, X-ray scatter would provide an important confirmation for life detection in the Wolf Trap device. The evidence of life would be much more conclusive if, concurrently with an increase in the number of particles, an increase in the number of particle subunits were also observed.

However, X-ray scatter is not a developed laboratory technique for detecting macromolecules within an organism. For this reason, testing is needed to determine the feasibility of this technique. The geometric considerations in X-ray scatter are very critical since the scatter angles are very small.

Mention has been made of the considerations necessary when designing a nutrient media to be used with X-rays. Such a media suitable for use with X-rays would also be suitable for

use with light, if one more criteria were met—transparency to light. Because losses in the incident beam of X-rays will occur in the windows as well as the nutrient, the path length in these materials is necessarily quite short.

To reduce this absorption, the windows must be constructed from materials of low atomic number, such as beryllium and aluminum. The same window might not pass both types of radiation as all common light transparent materials stop X-rays (except perhaps plastic).

One important feature of X-ray is that the photons are so energetic that single photons can be counted. Thus, the source intensity for X-ray scatter determinations can be low.

There are several possible X-ray sources that could meet the needs of a life detection instrument; for example miniature X-ray generators, or radioactive sources. The latter is especially attractive since such sources require no power. The feasibility of this approach depends, in part, on the concentration of macromolecules within an organism; i.e., if macromolecules are highly clumped, it is difficult to get meaningful data.

Laboratory measurements are needed to determine the optimum optics for X-ray scatter. Some of the considerations are known for light scatter, but more information is needed for the specific case of X-ray scatter.

The following is a list of suggestions for laboratory testing of the X-ray scatter technique.

(1) Conduct tests to determine whether radioactive X-ray sources will be suitable.

(2) Conduct tests to determine the suitability of currently available X-ray generators. It may be desirable, however, to develop and test an efficient, small X-ray generator with a highly collimated beam for this specific application.

(3) Test various media for use in Wolf Trap to optimize the X-ray scatter technique.

(4) Design an experimental culture cell that is practical for both light and X-ray scatter—if both techniques are to be used.

(5) Conduct further tests to relate the X-ray scatter technique to the other parameters being measured.

Section 3
CONDUCTIVITY

Hydrogen ion concentration measurement (pH) has already been suggested as a parameter to be measured in Wolf Trap; however, due to the existing problems of electrode sterilization, it is necessary to consider an alternate approach. Conductivity could give somewhat the same type of information as pH measurements. Once the sample is introduced and the system has stabilized, any changes in conductivity would be due to changes in temperature or chemical ionization.

Electricity has been shown to flow through liquids. This flow depends on the movement of electric charges such as: electrons (as in the case of metals); positive and negative ions (as in salt, acid or base solutions); or larger charged particles (as in colloidal conductors).

The current flowing through a given electrolytic conductor is related to: the applied voltage; the number of charged particles; and the current-carrying capacity of the particles in the solvent at a given temperature and pressure.

Chemical reactions occur at two metallic electrodes—an anode and a cathode. Anions, which are negative ions, move towards the anode while cations, which are positive ions, move towards the cathode. Conductance in an electrolytic cell involves both ionic and electronic transport. Electrons are released to the metal by ions at the anodes (oxidation). These electrons are transported to the cathode where electrons are absorbed from the electrode by ions (reduction).

Current is proportional to the applied electromotive force in metallic conduction.

$$I = \frac{V}{R} \qquad (3.1)$$

where I is the current, V the electromotive force, and R is the resistance of the circuit. This is Ohm's law. Frederick Kohlrausch has shown that this law also applies to electrolytic conductance when polarization (as defined below) is eliminated because an electrolyte has a constant resistance under given conditions.

If a direct current is driven between two platinum electrodes immersed in an electrolytic solution, the flow of current may decrease in time. Part of the explanation for this decrease in flow is found in the accumulation of the products of electrolysis at the electrodes. These products form a galvanic cell that causes a current to flow in the opposite direction of the primary flow. This reverse electromotive force is called the electromotive force of polarization.

In order to accurately measure electrolytic conductivity, polarization must be eliminated. In 1869, Kohlrausch and Molborn virtually eliminated polarization in their measurements by using an alternating rather than direct current. By this method, the ions are driven first in one direction and then the other. This allows only a small amount of the products of electrolysis to accumulate at the electrodes.

An additional approach for reducing polarization is the use of platinum black electrodes. This increases surface area—which is desirable; however, platinum electrodes absorb a certain amount of salt in the blacking process (immersion in a 3 percent solution of platinum chloride that contains a trace of lead acetate). This could introduce errors when dilute solutions are involved. To increase sensitivity in dilute solutions, the electrodes are heated after platinization to give a gray surface.

The usual method of measuring resistance is the Wheatstone bridge, which is diagramed below.

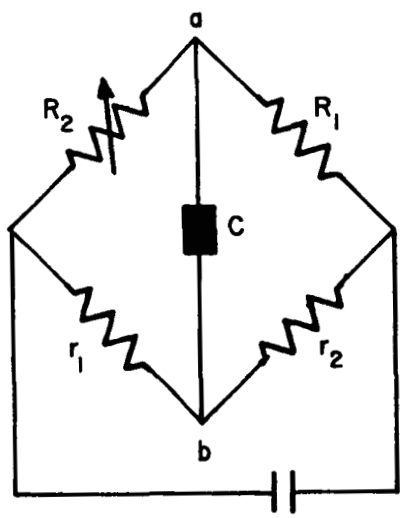

Fig. 3-1 Wheatstone Bridge

In this figure, r_1 and r_2 are fixed resistances with R_1 the electrolytic cell of unknown resistance. R_2 is a variable potentiometer that is adjusted until the detector C indicates that no current is flowing across the bridge. In this equilibrium condition, the voltage at points a and b are identical. Figure 3-2 shows a generalized electrolytic cell.

The resistance of the electrolyte is given by

$$R_1 = R_2 \frac{r_1}{r_2} \qquad (3.2)$$

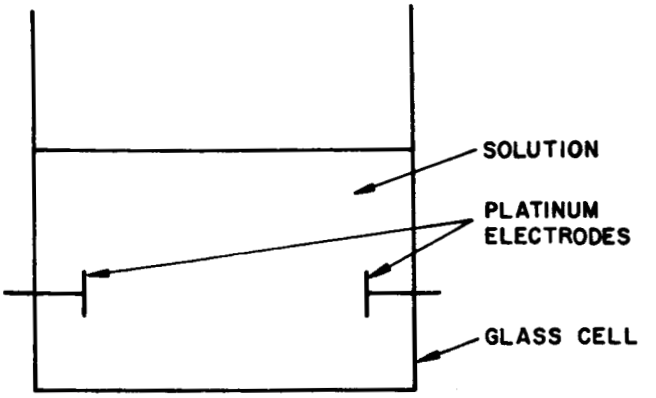

Fig. 3-2 Electrolytic Cell

The conductance is

$$\rho = \frac{1}{R_1} \qquad (3.3)$$

which is the current (in amperes) for 1 volt potential difference between the electrodes.

The cell is placed in a thermostatically controlled bath, since conductivity increases with temperature. For a standardized cell, the temperature coefficient is approximately 2 percent per degree.

Several alternate methods for measuring conductivity have been proposed, all of them using direct current. These approaches attempt to overcome errors introduced by electrostatic capacity

and polarization. E. Newberry modified the usual method of measuring resistance in a metallic conductor by determining, during the flow of a known current, the fall of potential between two points in a path of known dimensions. For this purpose, a tube of known dimensions contains the electrolyte. The tube is placed horizontally, connected at each end to vessels containing the electrodes. Standard electrodes (calomel, mercurous sulfate) come into contact with the solution in the tube at two intermediate points and connect with an accurate dial potentiometer. The resistance of the electrolyte is defined by Ohm's law. E. D. Eastman developed a similar method, but both methods are limited to electrolytes for which nonpolarizable electrodes are known.

The dimensions of a conductivity cell do not need to be known precisely if the cell is standardized with a solution of known conductivity. Thus, a cell constant can be found that relates the resistance of the cell to the conductivity of the solution. The conductivity of the solvent used is subtracted from the observed conductivity of the solution. (Low conductivity water may be obtained by using ion exchange resins or by distilling water twice in a block tin apparatus. The specific conductivity of such water is about 0.1×10^{-6} when contaminated with dissolved carbon dioxide.)

The equivalent conductivity of a solute (Λ) is defined as the specific conductance of the solution in $ohm^{-1}\ cm^{-1}$, divided by its concentration in equivalents per cubic centimeter.

$$\Lambda = \frac{1000k}{c} \qquad (3.4)$$

Kohlrausch demonstrated that this quantity increases with decreasing concentration, reaching a limiting value Λ_∞ at zero concentration. After studying the limiting values for a series of electrolytes, it was found that each ion contributes characteristically to conductivity. From this, then, is derived the law of independent mobilities.

$$\Lambda_\infty = \lambda_+^\circ + \lambda_-^\circ \qquad (3.5)$$

where λ_+° contributes the positive ions, and λ_-° the negative.

The limiting conductivity values are accordingly proportional to the mobilities (defined as velocities per volt per centimeter) of the ions u_+ and u_-, in accordance with the relation

$$\Lambda_\infty = \lambda_+^\circ + \lambda_-^\circ = K(u_+ + u_-) \qquad (3.6)$$

Since the mobility ratio $(u^+/u^+ + u^-)$ is equal to the ratio of the so called ionic transport number, which can be determined experimentally, the individual ionic conductances can also be calculated by combining conductance and transference measurements.

In 1887, Svante Arrhenius proposed the classical ionic or electrolytic dissociation theory. He was the first to assume that electrolytic conductance is due to freely moving charged particles. The limits of his theory are seen in his consideration of the implications of Eq. (3.4). Experiments have shown that as the concentration decreases, Λ increases. Arrhenius explained this by assuming that the number of ionic carriers decreases as the concentration decreases. Another of his

assumptions was that ionic mobility (the speed of ions in a field of 1 volt cm^{-1}) is independent of concentration. Because of these last two assumptions, Arrhenius's theoretical work is limited to the case of the weakly ionized solution (i.e. solutions of weak electrolytes).

In 1923, Debye and Hückel worked on an interionic attraction theory that would enable work to be done with strong electrolytes. According to their theory, a charged ion is surrounded by ions of opposite charge—an ion atmosphere. This is due to electrostatic (coulomb) forces and thermal motion.

The ion atmosphere, having a net charge equal to but opposite in sign from the sign of the central ion, moves with its associated molecules in the opposite direction of the central ion when an electric potential is applied. As a result, the central ion moves against a counter current of solvent, which amounts to an increase in viscous drag. This can be compared to the retarding effect of the solvent on the motion of colloidal particles in an electric field; hence, the name: electrophoretic effect.

If no external electric field is applied, a spherically symmetrical ion atmosphere exists, with the electrical center of gravity at the central ion. When an external field is applied, the ion atmosphere moves to compensate for this charge. This occurs rapidly, but not instantaneously. This phenomenon is called the time of relaxation.

The electrophoretic effect and the time of relaxation effect both increase as concentration increases; hence, the ions

move faster in a more dilute solution. Also, the equivalent conductivity* increases with dilution until—at infinite dilution—it reaches a constant value Λ_∞ . The theory shows that the equivalent conductivity Λ_∞ , which would occur if there were no interactions between the ions, is reduced to

$$\Lambda = \Lambda_\infty - a\sqrt{C} \tag{3.7}$$

where C is the concentration of ions and a is a constant.

Onsager developed an equation for quantitative conductance in very dilute solutions, based upon the aformentioned considerations

$$\Lambda = \Lambda_\infty - (\alpha\Lambda_\infty + \beta)\sqrt{C} \tag{3.8}$$

where C is the ion concentration, and the constants α and b depend on the nature of the solvent and upon the temperature. For univalent electrolytes,

$$\alpha = \frac{8.20 \times 10^5}{(DT)^{3/2}} \tag{3.9}$$

---

*The current in amperes flowing between two parallel electrodes 1 cm apart when the potential difference between the electrodes is one volt is defined as the electrical conductivity (Λ) when the cell contains 1 cm^3 of a solution containing 1 gram equivalent of electrolyte.

Kohlrausch stated in 1875 that the equivalent conductivity of an electrolyte at infinite dilution is the sum of two parts, one depending only on the cation and the other on the anion:

$$\Lambda_\infty = l_c + l_a$$

where l_c and l_a are called the mobilities of the ions expressed in equivalent conductivity units (ohm^{-1} cm^2).

and

$$\beta = \frac{82.4}{(DT)} \, 1/2n \qquad (3.10)$$

D being the dielectric constant at the absolute temperature T, and n being the viscosity. The Onsager equation has been shown correct for the conductance of strong electrolytes; however, deviations do occur as the concentration increases.

In 1934 Shedlovshky accounted for these deviations by extending Eq. (3.10) to

$$\Lambda_\infty = \Lambda'_\infty - AC - \beta C \log C + DC^2 \qquad (3.11)$$

in which

$$\Lambda'_\infty = (\Lambda + \beta\sqrt{C})/(I - \alpha\sqrt{C}) \qquad (3.12)$$

The last two terms may be omitted in many cases (for example, most univalent salts and strong acids in water up to a concentration of about 0.1 N). In 1957, R. M. Fuoss and Onsager took the size of the ions into consideration and proposed a theoretical explanation for the deviations. In 1954, R. H. Stokes and R. A. Robinson developed a semi-empirical equation that appears to hold true for conductance at high concentrations.

In 1927, M. Wien noted that the equivalent conductance of electrolytes increased at high potential gradients in accordance with the interionic attraction theory. The ion atmosphere hardly has time to form if the velocity of the ions resulting from high field strengths becomes great enough. The result is that both

the electrophoretic and time of relaxation effects become correspondingly diminished.

The interionic interference effects are more apparent at higher concentrations of high valence electrolytes. Unexpectedly, weak acids and bases show a large Wien effect. Consequently, it appears that high field strengths result in increased ionization in these weak electrolytes.

Generally, one measures conductance with alternating currents to avoid polarization. In 1928, Debye and Falkenhagen used frequencies greater than 5 mega-Hertz and demonstrated an increased equivalent conductance approaching a limiting value somewhat lower than Λ_∞ . At high frequencies, the ion atmosphere forms—as opposed to the Wien effect; however, because there is not enough time for the ions to fully distort, there is a loss of the time of relaxation effect. (The electrophoretic effect is not affected.) As the frequency is increased, Λ approaches $\Lambda_\infty - \beta\sqrt{C}$ rather than Λ_∞ .

In solvents of high dielectric constant, such as water, strong electrolytes appear completely ionized. However, in solvents of low dielectric constant, no strong electrolytes exist and large negative deviations from the Onsager slopes of conductance are observed.

When considering weak electrolytes, the following three assumptions must be made:

(1) Only a portion of a weak electrolyte is in the form of free ions

(2) The rest is undissociated

(3) An equilibrium exists between the two forms of the solute in accordance with the law of mass action. It is not necessary for the undissociated solute to consist of stable molecules bound together by chemical or quantum forces. N. Bjerrum suggested that they may be ion pairs; when a pair of ions of opposite charge are close together, electrostatic force tend to hold them together as a dipole. Such an ion pair may be separated if the average kinetic energy of the solvent molecule is greater than the potential energy of the ion pair; this is seen with strong electrolytes in solvents with high dielectric constants. In a solution having an average kinetic energy less than the mutual potential energy of the ion pair, the ion pair exists until it is struck by an exceptionally fast solvent molecule. By this theory, one can predict an increase in ion pairs if: the dielectric constant is low; the ions are small; the charges are large; and the temperature is low.

Arrhenius's dissociation theory demonstrated that weak electrolytes observed the Ostwald dilution law:

$$\Lambda = \Lambda_\infty - \frac{C\Lambda^2}{k\Lambda_\infty} \qquad (3.13)$$

where C equals concentration and k is a constant. This expression is based on the law of mass action and the following two

assumptions:

(1) The ions are perfect solutes

(2) The ratio $\frac{\Lambda}{\Lambda_\infty}$ represents the degree of dissociation.

Unfortunately, there are several complications. Assumption (1) is only an approximation of ionic behavior in dilute solutions, and assumption (2) is valid only if the mobility of ions do not change with concentration—which is contrary to fact.

Corrections for nonideal behavior of ion activity coefficients and for the decrease in ionic mobilities with increase in concentration have been made through the use of the interonic attraction theory of Debye, Hückel, and Onsager. In 1932, for example, MacInnes and Shedlovsky measured the conductance of aqueous acetic acid solutions and computed the ionization constant of this acid.

The above brief outline of the strong and weak electrolyte theory explains quantitatively the ionic conductivity in relatively dilute aqueous and nonaqueous solutions. The quantitative theory of colloidal solutions and concentrated ionic solutions is not yet complete in the literature.

The following effort is suggested to further evaluate the value of measuring this parameter in a life detection system:

(1) Design a culture chamber that meets the requirements of both light scatter and conductivity.

(2) Conduct studies to determine what types of media would best show a change in conductivity as a function of cellular growth.

(3) Conduct tests to determine the optimum electrode materials and forms (such as screens versus plates).

(4) Evaluate whether alternating or direct current best meets the requirements of the Wolf Trap life detection device.

(5) Conduct tests to determine how the electric current needed for this measurement would affect growing organisms.

(6) Study conductivity in relation to other parameters.

Section 4
FLUORESCENCE

Fluorescence is a property of matter involving the emissions of radiation as radiation is absorbed. When a solute particle is excited by the absorption of a photon, there are two possible paths by which the molecule can return to its lowest electronic state—its ground state.

One path is that of fluorescence. As the photon is absorbed, the electrons of the solute molecule are excited from the lowest vibrational level of the ground state to various vibrational levels of the excited singlet state. (The singlet state is one in which all of the electrons in the molecule have their spins paired.) Before an excited molecule can emit energy as a photon, it undergoes thermal relaxation, transferring the excess vibrational energy from the solute molecule to the solvent. The excess vibrational energy is the difference in energy between the various vibrational levels of the singlet state to which the molecule is excited and the lowest vibrational level of the singlet state from which energy is emitted. Energy is emitted as the molecule goes from the lowest vibrational level of the singlet state to various levels of the ground state (Fig. 4-1). (The energy absorbed can be either visible or ultraviolet light. The emitted light, the fluorescent light, is always a longer wavelength than is the absorbed light.)

The other path is referred to as intersystem crossing—a spin-dependent, internal conversion process that is not well understood. It is postulated that after the electrons are excited to the singlet state, there is a vibrational coupling between the excited singlet state and a triplet state. (The triplet state is defined as a state in which one set of electron spins has

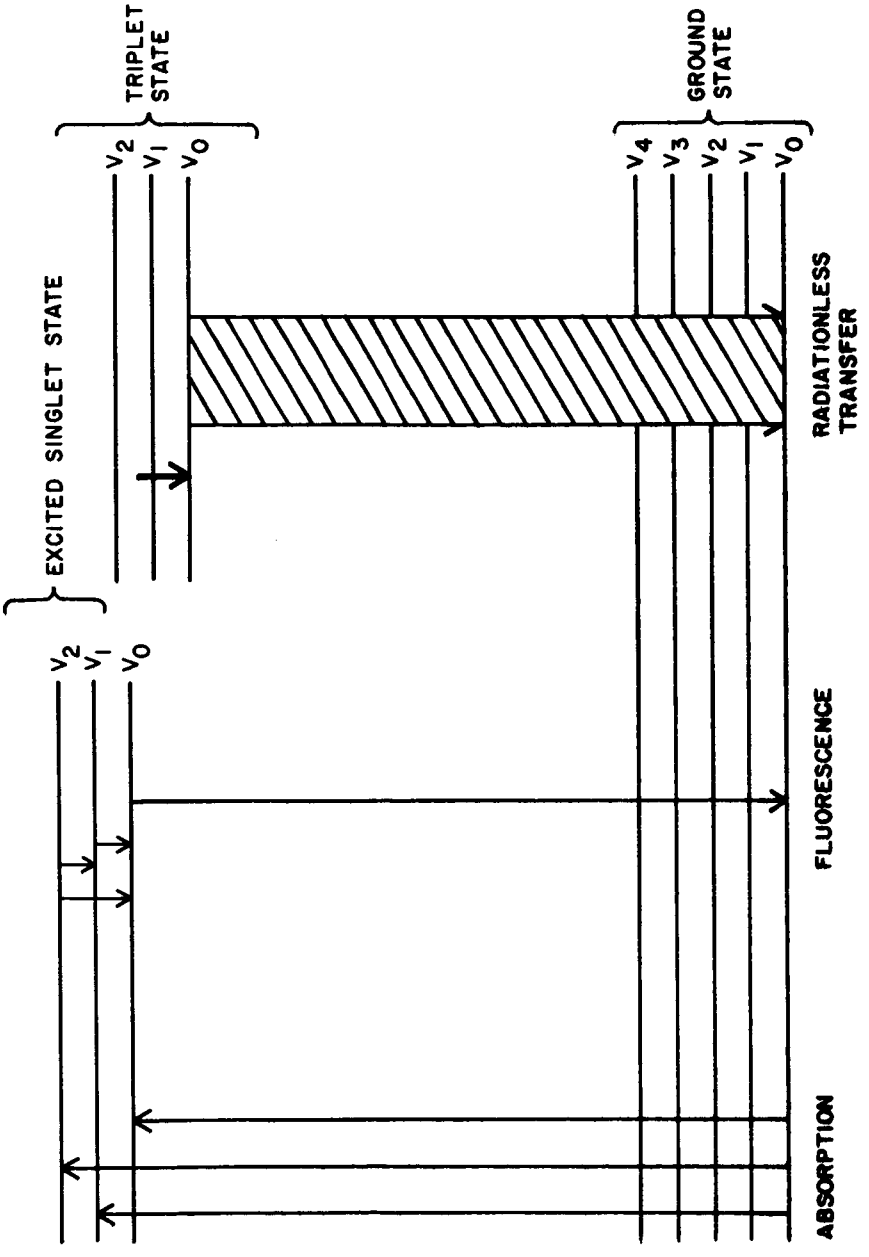

Fig. 4-1 Energy Level Diagram

become unpaired; i.e., all electrons in the molecule except two have paired spins.) Once the energy is trapped in the triplet state, it falls to the lowest vibrational level of the triplet state and then to the ground state. In this last step, the energy is converted to heat, and there is no emission of photons.

The fluorescence of a solute can be greatly affected by its external environment. Many solutes fluoresce only in select solvents; others fluoresce weakly in many solvents, brightly in only a few. Fluorescence is temperature dependent; an increase in temperature usually causes a decrease in fluorescence intensity. Some solutes are highly pH dependent, others are not. Inorganic salts, organic compounds, and dissolved gases can reduce the fluorescence properties of a compound in solution.

It is believed that all solutes without a triplet state do fluoresce. However, due to the efficient quenching agents such as water and dissolved O_2, it may be difficult to observe fluorescence in a solution. For example, substance X may be observed to fluoresce under a microscope, when the solute is suspended in a thin layer of solvent. The emitted light is easily observed, for the quenching effect of water and oxygen is low, due to the short distance the emitted light travels through the quenching medium. This same substance may show no fluorescence when the solution is observed in a test tube.

On the other hand, if the molecule does have a triplet state, there is no emission of radiation (the energy having been converted to heat.) The existence of a triplet state at present is rarely predictable. In many cases, it is only an observable phenomenon.

Fluorescence has been suggested as an additional parameter to be measured by the Wolf Trap device. Both X-ray and ultraviolet light could serve as an energy source for such work. However, the practicality of this method is debatable since fluorescence is not a fundamental property of all living matter. Furthermore, naturally occurring minerals and other nonliving materials fluoresce.

There are two possible approaches to measuring fluorescence: the organisms can be observed either in a culture chamber or under a microscope. However, because the volume of the culture chamber is great, the effect of possible quenching agents is also great.

On the other hand, the optics involved in a microscopic device are quite complex due to the number of lenses that are required. However, even if it were possible to view the organisms under conditions similar to ultraviolet microscopy, there would still be two problems: unknown substances would be introduced into the culture chamber along with the sample, in all likelihood affecting the fluorescence properties of the organisms; and there could well be serious instrumentation problems. The human eye is much more selective than detectors in discriminating between two light intensities; i.e., in detecting white on white, a star against sky glow, or small color differences. And the human eye can be dark adapted to discern as few as a 100 photons. At present, light detectors can do none of these things as well.

We suggest the following effort to determine the feasibility of measuring fluorescence in Wolf Trap:

(1) Evaluate X-ray generators as a source of the exciting energy.

(2) Study the practicality of ultraviolet as the exciting energy.

(3) Make instrument measurements on thin layers of nutrient suspensions.

(4) Consider the possible use of a fluorescent dye in colorimeter tests.

Section 5
COMPONENTS

Many engineering advances have recently been made in the components available to the designers of the Wolf Trap engineering model. It is desirable to remain aware of these advances so that the latest information will be available when the final design effort is required.

The following is a summary of recent developments in the components of special interest to us.

Energy Sources

(1) Manufacturers of incandescent lamps have recently built miniature lamps with a significant increase in reliability, shelf life, and life expectancy. These manufacturers have found a way to reduce the buildup of deposits on the windows and have developed a glass without the previous defect of discoloration (which is due to aging).

(2) Gallium arsenide infrared sources are now on the market. These rugged, stable, long-life devices are sources of highly collimated radiation. They are of interest because they provide useful intensities at moderate power requirements.

(3) Manufacturers have continued to improve the stability of glow discharge lamps and arc lamps. These lamps are available in a wide variety of emission frequencies; furthermore, they can be pulsed at high intensities.

(4) An interesting possibility at present is the use of radioactive light sources. Radioactive light requires no power, is very stable, and is available in a wide range of spectral outputs. However, the output is very weak and is also uncollimated. High gain detectors would have to be used.

(5) Radioactive X-ray sources are available for several different energies. Unfortunately, the commercial market offers no small X-ray generators with reasonable power requirements. Because of the unique requirements of Wolf Trap, it may be desirable to optimize the design of a special miniature generator.

Windows

(6) Corning Glassworks has recently marketed an optical window glass with high transmission efficiency for infrared light.

(7) Mention must be made of fused silica and sapphire windows. Due to recent improvements, the optical grade of these windows now approaches the requirements for coronograph optics. They are designed to be used primarily with ultraviolet light.

(8) High strength glass is now available for the manufacture of essentially indestructible laboratory glassware.

(9) High strength, low z windows are now marketed as thin films. These windows are able to pass both X-rays and a wide range of wavelengths in the visible spectrum.

(10) Researchers are continuing to improve beryllium windows for use with X-ray radiation.

(11) Currently available are rugged narrowband pass filters that allow selected frequencies of light to be observed, even though the light source is broadband.

Detectors

(12) Recent advances in silicon crystal detectors have increased sensitivity and decreased noise level in these instruments. Extremely rugged models are now available.

(13) Now on the market is a photosenstive N-channel silicon junction field effect transistor.

(14) Miniature gas-filled proportional counters are now available from several manufacturers. These counters have thin beryllium windows that efficiently pass X-ray radiation. Several models have already flown on rocket and satellite experiments.

(15) Within the year, another device of interest, the channeltron, is to be flight tested in satellite experiments. These devices are windowless light and particle sensitive distributed stage multipliers.

(16) Bell Laboratories has recently developed a germanium avalanche electron multiplier for use with visible and infrared light.

(17) Recently developed by Johnstone Laboratories is a mesh-grid electron multiplier. The multiplier can be used with ultraviolet and X-ray radiation. The exciting feature of this instrument is that—in addition to being lightweight and rugged—it can be sterilized (Maximum, 400°C in a vacuum).

Others

(18) It is possible to be increasingly more sophisticated in signal selection and interference rejection because large improvements are continuously being made in the fields of electron stability and noise level efficiency.

Section 6
CONCLUSIONS

The following conclusions result from our review of the literature on light scattering and previous work with the engineering model of Wolf Trap:

(1) The present laboratory research applications of X-ray scattering are much more refined than is needed in Wolf Trap. We must now set up a testing program to fully evaluate the data available from an instrument capable of being flown.

(2) A series of tests must be conducted to better understand the nature of conductivity measurements for biological systems. Also, conductivity must be studied in relation to the types of media being considered for Wolf Trap. In short, conductivity must be studied in light of its relationship to all other parameters on the Wolf Trap device.

(3) The requirements for measuring fluorescence must be studied to better judge its potential contribution within the available space and weight of the Wolf Trap device.

Continued testing should be conducted to refine and select those methods that will most effectively insure that the data obtained by the Wolf Trap device is conclusive.

Section 7
BIBLIOGRAPHY

E. H. Anderson, "Heat Reactivation of Ultra-Violet Inactivated Bacteria", Journal of Bacteriology, Vol. 61, pp 389 to 397, 1951

P. A. Anderson, "Automatic Recording of Growth Rates of Continuously Cultured Micro-Organisms", Journal of General Physiology, Vol. 36, pp 733 to 737, 1953

W. H. Aughey and F. J. Baum, "Angular-Dependence Light Scattering-A High - Resolution Recording Instrument for the Angular Range 0.05 - 140°", Journal of the Optical Society of America, Vol. 44, pp 833 to 837, 1954

F. J. Baum and F. W. Billmeyer, "Automatic Photometer for Measuring the Angular Dissymmetry of Light Scattering", Journal of the Optical Society of America, Vol. 51, pp 452 to 456, 1961

H. Benoit, "On the Effect of Branching and Polydispersity on the Angular Distribution of the Light Scattered by Gaussian Coils", Journal of Polymer Science, Vol. 11, pp 507 to 510, 1953

M. A. Blokhin, Methods of X-Ray Spectroscopic Research, Pergamon Press, 1965

R. H. Boll, R. O. Gumprecht and C. M. Sliepcevich, "Theoretical Light-Scattering Coefficients for Relative Refractive Indexes Less Than Unity and for Totally Reflecting Spheres", Journal of the Optical Society of America, Vo. 44, pp 18 to 21, 1954

J. H. Brewer and D. L. Allgeier, "Safe Self-Contained Carbon Dioxide-Hydrogen Anaerobic System", Applied Microbiology, Vol. 14, pp 985 to 988, 1966

R. F. Chen, G. G. Vurek and N. Alexander, "Fluorescence Decay Times: Proteins, Coenzymes, and Other Compounds in Water", Science, Vol. 156, pp 949 to 951, 1967

Chiao-Min Chu and S. W. Churchill, "Representation of the Angular Distribution of Radiation Scattered by a Spherical Particle", Journal of the Optical Society of America, Vol. 45, pp 958 to 962, 1955

G. C. Clark, Chiao-Min Chu and S. W. Churchill, "Angular-Distribution Coefficients for Radiation Scattered by a Spherical Particle", Journal of the Optical Society of America, Vol. 47, pp 81 to 84, 1957

M. K. Coultas and D. J. Hutchison, "Use of a Biophotometer in Growth-Curve Studies", Journal of Bacteriology, Vol. 83, pp 393-to 401, 1962

P. Doty and R. F. Steiner, "Light Scattering and Spectrophotometry of Colloidal Solutions", Journal of Chemical Physics, Vol. 18, pp 1211 to 1220, 1950

R. W. Fessenden and R. S. Stein, "On the Absolute Turbidity of Water", Journal of Chemical Physics, Vol. 22, pp 1778 to 1779, 1954

M. S. Fox and L. Szilard, "A Device for Growing Bacterial Populations Under Steady State Conditions", Journal of General Physiology, Vol. 39, pp 261 to 266, 1955

P. H. Frank and R. Ullman, "Determination of Dissymmetry of Scattering in Colored Solutions", Journal of the Optical Society of America, Vol. 45, pp 471 to 476, 1955

S. B. Gibson and D. J. Horowitz, Characteristics of Gallium Arsenide Diodes as Infrared Radiation Sources, U. S. Army Engineer Research and Development Laboratories, Report 1831, 1965

D. A. I. Goring and P. G. Napier, "Light Scattering Determination of the Absolute Turbidity of Water", Journal of Chemical Physics, Vol. 22, p 147, 1954

F. T. Gucker and S. H. Cohn, "Numerical Evaluation of the Mie Scattering Functions; Table of the Angular Functions π_n and τ_n of Orders 1 to 32, at 2.5° Intervals", Journal of Colloid Science, Vol. 8, pp 555 to 575, 1953

R. O. Gumprecht and C. M. Sliepcevich, "Measurement of Particle Sizes in Polydispersed Systems by Means of Light Transmission Measurements Combined with Differential Setting", Journal of Physical Chemistry, Vol. 57, pp 95 to 97, 1953

R. O. Gumprecht and C. M. Sliepcevich, "Scattering of Light by Large Spherical Particles", Journal of Physical Chemistry, Vol. 57, pp 90 to 95, 1953

D. H. Harris, "Martian Relief and the Coming Opposition", Science, Vol. 155, pp 1100 to 1101, 1967

P. G. W. Hawksley, "The Physics of Particle Size Measurement: Part II, Optical Methods and Light Scattering", The British Coal Utilization Research Association Bulletin, Vol. 16, pp 117 to 147, and 181 to 209, 1952

W. Heller, "Elements of the Theory of Light Scattering. I., Scattering in Gases, Liquids, Solutions, and Dispersions of Small Particles", Record of Chemical Progress, Vol. 20, pp 208 to 233, 1959

J. R. Hodkinson, "Particle Sizing by Means of the Forward Scattering Lobe", Applied Optics, Vol. 5, pp 840 to 844, 1966

N. H. Horowitz, "The Search for Extraterrestrial Life", Science, Vol. 151, pp 789 to 792, 1966

M. M. Hugue, J. Jaworzyn and D. A. I. Goring, "Ultraclarification of Solutions for Light-Scattering Measurements", Journal of Polymer Science, Vol. 39, pp 9 to 20, 1959

M. C. Van de Hulst, Light Scattering by Small Particles, John Wilsy & Sons, Inc., New York, 1957

B. Jacobson and B. Lindberg, "X-Ray Spectrophotometer for Simultaneous Analysis of Several Elements", The Review of Scientific Instruments, Vol. 35, pp 1316 to 1319, 1964

H. G. Jerrard and D. B. Sellen, "A New Apparatus for Light Scattering Studies", Applied Optics, Vol. 1, pp 243 to 247, 1962

L. A. Kamentsky, "Spectrophotometer: New Instrument for Ultrarapid Cell Analysis", Science, Vol. 150, pp 630 to 631, 1965

M. Kerker, W. A. Farone, L. B. Smith and E. Matyević, "Determination of Particle Size by the Minima and Maxima in the Angular Dependence of the Scattered Light Range of Validity of the Method", Journal of Colloid Science, Vol. 19, pp 193 to 200, 1964

M. F. Kerker, W. A. Farone and E. Matyevic, "Applicability of Rayleigh-Gans Scattering to Spherical Particles", Journal of the Optical Society of America, Vol. 53, pp 758 to 759, 1963

S. Kitani, "Measurement of Particle Sizes by Higher Order Tyndall Spectra (θ_1 , Method)", Journal of Colloid Science, Vol. 15, pp 237 to 293, 1960

S. Koga and T. Fujita, "Anomalous Light Scattering by Microbial Cell Suspensions", Journal of General Applied Microbiology, Vol. 8, pp 223 to 232, 1962

B. Kok and J. E. Varner, "Extraterrestrial Life Detection Based on Oxygen Isotope Exchange Reactions", Science, Vol. 155, pp 1110 to 1112, 1967

J. P. Krathovil, Gj. Dezelic, M. Kerker and E. Matijevic, "Calibration of Light-Scattering Instruments: A Critical Survey", Journal of Polymer Science, Vol. 57, pp 59 to 78, 1962

J. Kraut and W. B. Dandliker, "Light Scattering by Water", Journal of Chemical Physics, Vol. 23, pp 1544 to 1545, 1955

M. J. Kronman and S. N. Timasheff, "A Light-Scattering Cell for Angular Measurements", Journal of Polymer Science, Vol. 137, pp 573 to 576, 1959

L. M. Kushner, "A Design for an Absolute Light-Scattering Photometer", Journal of the Optical Society of America, Vol. 44, pp 155 to 157, 1954

R. A. MacLeod, M. Light, L. A. White and J. F. Currie, "Sensitive Rapid Detection Method for Viable Bacterial Cells", Applied Microbiology, Vol. 14, pp 979 to 984, 1966

H. P. Mausberg, Y. Y. Yamagamai and C. Berkley, "Spot Scanner Counts Micron-Sized Particles", Electronics, Vol. 30, pp 142 to 146, 1957

S. H. Maron and M. E. Elder, "Determination of Latex Particle Size by Light Scattering. I., Minimum Intensity Method", Journal of Colloid Science, Vol. 18, pp 107 to 118, 1963

S. H. Maron, P. E. Pierce and M. E. Elder, "Determination of Latex Particle Size by Light Scattering. II L, Minima and Maxima in Angular Dependence of Intensity", Journal of Colloid Science, Vol. 18, pp 391 to 399, 1963

D. McIntyre, "An Absolute Light Scattering Photometer: II. Direct Determination of Scattered Light from Solutions", Journal of Research of the National Bureau of Standards, Vol. 68A, pp 87 to 96, 1964

D. McIntyre and G. C. Doderer, "Absolute Light-Scattering Photometer: I. Design and Operation", Journal of Research of the National Bureau of Standards, Vol. 62, pp 153 to 159, 1959

W. B. Mercer, "Calibration of Coulter Counters for Particles 1μ in Diameter", Review of Scientific Instruments, Vol. 37, pp 1515 to 1520, 1966

L. Packer and M. Perry, "Energy-Linked Light-Scattering Changes in Escherichia coli", Archives of Biochemistry and Biophysics, Vol. 95, pp 379 to 388, 1961

L. Packer and W. Vishniac, "Chemosynthetic Fixation of Carbon Dioxide and Characteristics of Hydrogenase in Resting Cell Suspensions of Hydrogenomonas ruhlandu nov. spec", Journal of Bacteriology, Vol. 10, pp 216 to 223, 1955

R. B. Penndorf, "Approximation Formula for Forward Scattering", Journal of the Optical Society of America, Vol. 52, pp 797 to 800, 1962

R. B. Penndorf, "New Tables of Total Mie Scattering Coefficients for Spherical Particles of Real Refractive Indexes ($1.33 \leq n \leq 1.50$)", Journal of the Optical Society of America, Vol. 47, pp 1010 to 1015, 1957

C. J. Perret, "An Apparatus for the Continuous Culture of Bacteria at Constant Population Density", Journal of General Microbiology, Vol. 16, pp 250 to 264, 1957

E. Peters and J. J. Byerley, "High Pressure Spectrophotometric Cell", Review of Scientific Instruments, Vol. 34, pp 819 to 820, 1963

M. J. Pine and W. Vishniac, "The Methane Fermentations of Acetate and Methanol", Journal of Bacteriology, Vol. 73, pp 736 to 742, 1957

M. L. Polyanyi, "Volume and Index Measurements of Blood Cells with a Recording Diffractometer", The Review of Scientific Instruments, Vol. 30, pp 626 to 632, 1959

F. H. Quimby, (Ed.), Concepts for Detection of Extraterrestrial Life, NASA SP-56, 1964

C. Sadron, "Methods of Determining the Form and Dimensions of Particles in Solution: A Critical Survey", Progress in Biophysics and Biophysical Chemistry, Vol. 3, pp 237 to 304, 1953

K. Shibata, A. A. Benson and M Calvin, "The Absorption Spectra of Suspensions of Living Micro-Organisms", Biochimica et Biophysica Acta, Vol. 15, pp 461 to 470, 1954

B. A. Silverman, B. J. Thompson and J. H. Ward, "A Laser Fog Disdrometer", Journal of Applied Meterology, Vol. 3, pp 792 to 801, 1964

J. L. Stokes and M. L. Redmond, "Quantitative Ecology of Psychrophilic Micro-Organisms", Journal of Applied Microbiology, Vol. 14, pp 74 to 78, 1966

R. Teucher, "Optisches Teilchengrobenspektrometer", Dechema Monograph, Vol. 44, pp 83 to 89, 1963

A. Turkevich, K. Knolle, R. A. Emmer, W. A. Anderson, J. H. Patterson and E. Franzgrote, "Instrument for Lunar Surface Chemical Analysis", The Review of Scientific Instruments, Vol. 37, pp 1781 to 1786, 1966

G. K. Turner, "An Absolute Spectrofluorometer", Science, Vol. 146, pp 183 to 189, 1964

J. Vilms, L. Wandinger and K. L. Klohn, "Optimization of the Gallium Arsenide Injection Laser for Maximum Power Output", Technical Report Ecom-2613, 1965

W. Vishniac, "Biochemical Aspects of Photosynthesis", Annual Review of Plant Biochemistry, Vol. 6, pp 115 to 134, 1955

W. Vishniac, "Extraterrestrial Microbiology", Aerospace Medicine, Vol. 31, pp 678 to 680, 1960

W. Vishniac, "Photochemical Reduction of Pyridine Nucleotides", American Society of Biological Chemists, Vol. 10, p 265, 1951

W. Vishniac and S. Ochoa, "Fixation of Carbon Dioxide Couplet to Photochemical Reduction of Pyridine Nucleotides by Chloroplast Preparations", Journal of Biological Chemistry, Vol. 195, pp 75 to 93, 1952

W. Vishniac and S. Ochoa, "Photochemical Reduction of Pyridine Nucleotides by Spinach Grana and Coupled Carbon Dioxide Fixation", Nature, Vol. 167, pp 768 to 769, 1951

W. Vishniac and I. A. Rose, "Mechanism of Chlorophyll Action in Photosynthesis", Nature, Vol. 182, pp 1089 to 1090, 1958

R. A. Wells and G. Fielder, "Martian and Lunar Craters", Science, Vol. 155, pp 357 to 355, 1967

C. Wippler and G. Scheibling, "Description d'un Appareil Pour L'Etude de la Diffusion de la Lumiere", Journal of Chemical Physics, Vol. 51, pp 201 to 205, 1954

Jen Tsi Yang, "An Improvement in the Graphic Treatment of Angular Light Scattering Data", Journal of Polymer Science, Vol. 26, pp 305 to 310, 1957

B. H. Zimm, "Apparatus and Methods for Measurement and Interpretation of the Angular Variation of Light Scattering; Preliminary Results on Polystyrene Solutions", Journal of Chemical Physics, Vol. 16, pp 1099 to 1116, 1948